Available online at www.sciencedirect.com
SCIENCE DIRECT®
International Journal of Heat and Fluid Flow 24 (2003) 236–241
International Journal of HEAT AND FLUID FLOW
www.elsevier.com/locate/ijhff

Friction factor at low Knudsen number for the duct with sine-shaped cross-section

Ombretta Pinazza [a], Marco Spiga [b,*]

[a] INFN, Viale Irnerio 46, 40126 Bologna, Italy
[b] Department of Industrial Engineering, University of Parma, Parco Area delle Scienze, 43100 Parma, Italy

Received 4 March 2002; accepted 8 August 2002

Abstract

A numerical method is applied to analyse hydrodynamically developed internal forced laminar flow in microgeometries, for a Newtonian fluid in ducts of sinusoidal cross-section. The solution to the momentum equation is obtained through a co-ordinate transformation that maps the sinusoidal cross-section into the interior of a square. The hypotheses of constant physical properties and fully isothermal developed flow are supposed to hold. Slip flow conditions are imposed at the walls, with a first-order boundary condition. The effects of the fluid rarefaction appear in the Knudsen number, which introduces the linear dependence between the slip velocity and the velocity gradient. The 2D velocity distribution is obtained as a function of the Knudsen number, and consequently, the friction factor (in fully developed isothermal flow) is deduced.

Keywords: Friction factor; Sine-shaped cross-section; Slip-flow; Fluid-dynamics

1. Introduction

The cooling of microelectronics and microstructures is becoming more and more crucial with the increasing downscaling of integrated circuits and the growth of the micromachining industry. Microelectromechanical systems (MEMS) can sense, control and actuate devices in several applications, they are fabricated in long arrays and can range in size from micrometres to millimetres Ho and Tai (1996). Miniaturisation of mechanical systems enables great opportunity in the progress of science and technology; they are lighter, faster and more precise than their macroscopic counterparts.

Research on MEMS is exploring design tools to facilitate the conception of these microstructures, mainly for packaging solutions. Many applications involve the analysis of fluid flow in microscale geometry, ranging from microsurgery and microinstrumentation, to minuscule robots. Other applications include micropumps, miniature heat pumps, injectors, microheat exchangers, propulsion of microsatellites, transport of gases in microchromatography, biomedical technologies, ink-jet printer heads. Thermal issues are crucial at all levels of product hierarchy.

In electronic cooling the circuits are located on one side of the wafer, whereas microchannels are fabricated on the other side. Due to the small hydraulic diameter, often the fluid has low Reynolds number and turbulence is not desired for obvious drag and noise problems.

On the microscale, fluid flow is strongly affected by surface phenomena. The inertial forces tend to be small, and surface effects are prevailing; in a non-negligible layer molecular collisions with the wall dominate over intermolecular collisions, while the bulk of the fluid maintains its continuum behaviour. In several applications the flow pattern corresponds to a slip flow, the fluid presents a loss of adhesion at the wetted wall making the fluid slide along the wall. Slip in internal flows occurs for gas at low pressure and for flow in small passages. This effect has a tremendous influence on pressure drop, shear stress, mass flow rate, and the physical laws governing fluid flow models differ from the classical laws of continuum fluid dynamics.

The appropriate flow models depend on the range of the Knudsen number. For $Kn < 10^{-3}$ the fluid can be considered as a continuum, for $10^{-3} < Kn < 0.1$ slip

* Corresponding author. Tel.: +39-521-905855; fax: +39-521-905705.
E-mail address: macro.spiga@unipr.it (M. Spiga).

0142-727X/03/$ - see front matter © 2002 Elsevier Science Inc. All rights reserved.
doi:10.1016/S0142-727X(02)00221-7

Nomenclature

A	cross-sectional area of the duct, m^2
a, b	typical dimensions of the sinusoidal cross-section, m
d	dimensionless hydraulic diameter of the duct D/a
D	hydraulic diameter of the duct $4A/P_w$, m
f	Darcy–Weisbach friction factor in fully developed isothermal flow
g_ζ	ζ-component of the gravitational acceleration, $m\,s^{-2}$
J	Jacobian
Kn	hydraulic-diameter based Knudsen number λ/D
n	dimensionless co-ordinate normal to the perimeter contour, entering the fluid core
p	pressure, Pa
P	velocity defined in Eq. (3), $m\,s^{-1}$
P_w	wetted perimeter, m
Re	Reynolds number WD/v
t	dimensionless shear stress
U	dimensionless average fluid velocity W/P
$v(\cdot)$	dimensionless fluid velocity V/P
$V(\cdot)$	axial fluid velocity, $m\,s^{-1}$
W	average velocity, $m\,s^{-1}$
x, y, z	dimensionless rectangular Cartesian co-ordinates in the physical domain
x', y'	dimensionless transformed Cartesian co-ordinates in the computational domain

Greeks

α	slip coefficient
β	sine aspect ratio b/a
λ	mean free path, m
μ	dynamic viscosity, Pa s
ρ	density, $kg\,m^{-3}$
τ	shear stress, Pa
ξ, η, ζ	Cartesian co-ordinates, m

Subscripts

max	maximum
w	wall
x or y	derivation with respect the co-ordinate x or y

flow is observed, it occurs when the fluid velocity on the wall differs from the wall velocity and the molecular mean free path becomes comparable with the tube hydraulic diameter. For increasing Knudsen number, $0.1 < Kn < 10$, a transition regime is observed, for $Kn > 10$ the fluid is in free molecular flow.

The classification is based on empirical information and it could be modified according to the flow geometry, as verified by Tison (1993), who found that in a pipe the slip flow regime extends up to $Kn = 0.6$. An exhaustive review is reported in Beskok et al. (1996) and Karniadakis and Beskok (2001).

Numerical simulation is well suited for microflows. In the slip flow regime the Navier–Stokes equation can be used, involving either modified boundary conditions at the surface, or modified transport coefficients. Slip flow in circular and rectangular ducts has been already analysed (Barron et al., 1997; Larrodé et al., 2000; Kwang-Hua, 1999; Morini and Spiga, 1998), but the flow passages in microheat exchangers and cooling devices can present a different geometry.

With the advancement of technology many different passage configurations have been introduced; one of the most interesting geometry, for its recent practical applications, is the sinusoidal cross-section (Manglik and Bergles, 1998; Ding and Manglik, 1996; Uzun and Ünsal, 1997). It can be found as a passage represented by a single sine curve forming the upper portion of the duct and a flat plate at the bottom portion of the boundary. These ducts represent a typical corrugated profile, common in compact heat exchangers because of their simplicity of construction, where they provide larger surface area and small hydraulic diameters, promoting a better heat transfer condition. The sinusoidal shape is originated by the effort to obtain triangular passages, when, due to manufacturing processes, rounded corners are obtained. The small hydraulic diameter of the sinusoidal ducts allows obtaining a low Reynolds number; hence fully developed laminar flow can prevail along the tube length. Several papers have reported solutions for continuum laminar flow in sinusoidal ducts and the research interest is significant, as discussed by Pinazza and Spiga (2000) and Richardson et al. (2000). The pioneering numerical works were reviewed and presented by Shah and London (1978), concerning the single sine shape geometry, but recent papers presented new contributions and higher accuracy in the numerical results.

The aim of this paper is the numerical analysis of the main dynamic parameters involved in slip flow of Newtonian fluids in single sine-shaped ducts. The paper presents a comparison between the computed parameters (as a function of the Knudsen number) and the analogous data, available in references only for $Kn = 0$.

The results constitute an original development in the field of basic microfluid dynamics and could provide a new tool for applications to engineering problems in miniaturisation.

2. Fluid flow and duct geometry

A single phase, Newtonian fluid is considered in steady-state, hydrodynamically developed forced laminar slip flow in a single-sine-shaped duct, schematically shown in Fig. 1. The Cartesian system of co-ordinates ξ, η, ζ has its origin in the centre of the straight line, with ξ along the horizontal side a, ζ perpendicular to the cross-section, $\eta = (1/2)b(1 + \cos 2\pi\xi/a)$.

The cross-sectional area can be easily evaluated; in dimensionless form (A/a^2) it results $\beta/2$, while the dimensionless wetted perimeter can be numerically determined by solving the following integral:

$$\frac{P_w}{a} = 1 + 2\int_0^{1/2} \sqrt{1 + \beta^2\pi^2 \sin^2(2\pi x)}\, dx \tag{1}$$

Introducing the usual hypotheses of constant physical properties and pressure gradient along the ζ axis, and neglecting natural convection and viscous dissipation, the dimensionless momentum Navier–Stokes equation is:

$$\frac{\partial^2 V}{\partial x^2} + \frac{\partial^2 V}{\partial y^2} + 1 = 0 \tag{2}$$

The dimensionless co-ordinates and velocity are:

$$x = \frac{\xi}{a}\left(-\frac{1}{2} \leqslant x \leqslant \frac{1}{2}\right), \quad y = \frac{\eta}{a}, \quad v = \frac{V}{P} \quad \text{with}$$
$$P = \frac{a^2}{\mu}\left(-\frac{\partial p}{\partial \zeta} + \rho g_\zeta\right) \tag{3}$$

The co-ordinate y ranges from 0 to $(1/2)\beta[1 + \cos(2\pi x)]$. To obtain a well-posed partial differential problem, the slip boundary conditions are prescribed as:

$$v_w = \alpha dKn\left(\frac{\partial v}{\partial n}\right)_w \tag{4}$$

where the coefficient α depends on properties of the interaction between gas and wall surface through the accommodation coefficients (Barron et al., 1997; Larrodé et al., 2000); $\alpha = 1$ corresponds to diffuse scattering, as typical in engineering applications. Hence, hereafter α will be considered unity. The strong coupling of the governing equations and more general non-linear boundary conditions make the problem very intensive, computationally.

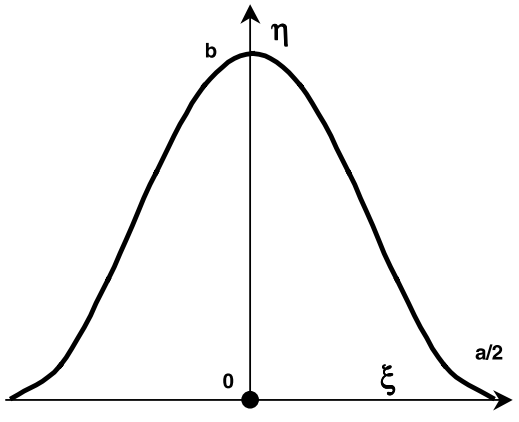

Fig. 1. Co-ordinates for the sine-shaped duct cross-section.

3. Numerical procedure

The numerical solution is obtained by transforming the sine-shaped cross-section into an equivalent square computational domain. Resorting to the grid generation technique, the differential equation (2) is transformed from the physical domain in the (x, y) plane to the computational domain in the (x', y') plane (Hornbeck, 1975; Haltiner and Williams, 1980; Thomson et al., 1982). The new transformed equation is solved on a rectangular grid in the computational plane, whose co-ordinates are chosen to satisfy the Laplace equation:

$$\frac{\partial^2 x'}{\partial x^2} + \frac{\partial^2 x'}{\partial y^2} = 0 \quad \frac{\partial^2 y'}{\partial x^2} + \frac{\partial^2 y'}{\partial y^2} = 0 \tag{5}$$

The sinusoidal surface contour is mapped into a square. The straight line becomes two consecutive sides of the square, the sinusoidal line is represented by the other two sides of the square. According to the numerical procedure, using the chain rule, the partial derivatives become:

$$\begin{aligned}
\frac{\partial}{\partial x} &= x'_x\frac{\partial}{\partial x'} + y'_x\frac{\partial}{\partial y'}\frac{\partial}{\partial y} = x'_y\frac{\partial}{\partial x'} + y'_y\frac{\partial}{\partial y'} \\
\frac{\partial^2}{\partial x^2} &= x'_{xx}\frac{\partial}{\partial x'} + y'_{xx}\frac{\partial}{\partial y'} + x'^2_{x}\frac{\partial^2}{\partial x'^2} + 2x'_x y'_x\frac{\partial}{\partial x'}\frac{\partial}{\partial y'} + y'^2_{xx}\frac{\partial^2}{\partial y'^2} \\
\frac{\partial^2}{\partial y^2} &= y'_{yy}\frac{\partial}{\partial y'} + y'_{yy}\frac{\partial}{\partial y'} + x'^2_{yy}\frac{\partial^2}{\partial x'^2} + 2x'_y y'_y\frac{\partial}{\partial x'}\frac{\partial}{\partial y'} + y'^2_{yy}\frac{\partial^2}{\partial y'^2}
\end{aligned} \tag{6}$$

The partial derivatives of an arbitrary function u (with respect to x and y, respectively) are:

$$u_x = u_{x'}x'_x + u_{y'}y'_x \quad u_y = u_{x'}x'_y + u_{y'}y'_y \tag{7}$$

The correlations among the derivatives of the physical and transformed co-ordinates are:

$$\begin{aligned}
&x_{x'}x'_x + x_{y'}y'_x = 1, \quad x_{x'}x'_y + x_{y'}y'_y = 0, \\
&y_{x'}x'_x + y_{y'}y'_x = 0, \quad y_{x'}x'_y + y_{y'}y'_y = 1
\end{aligned} \tag{8}$$

being $x_x = y_y = 1$, $x_y = y_x = 0$.

By solving the system (8), the unknown derivatives are expressed as:

$$x'_x = \frac{y_{y'}}{J}, \quad y'_x = -\frac{y_{x'}}{J}, \quad x'_y = -\frac{x_{y'}}{J}, \quad y'_y = \frac{x_{x'}}{J} \tag{9}$$

where J is the Jacobian of the transformation $J = x_{x'}y_{y'} - x_{y'}y_{x'}$. The Jacobian of the transformation is always non-zero.

The grid generation is performed through the conformal transformation governed by the equations:

$$(x_{y'}^2 + y_{y'}^2)\frac{\partial^2 x}{\partial x'^2} - 2(x_{x'}x_{y'} + y_{x'}y_{y'})\frac{\partial^2 x}{\partial x'\partial y'} + (x_{x'}^2 + y_{x'}^2)\frac{\partial^2 x}{\partial y'^2} = 0,$$
$$(x_{y'}^2 + y_{y'}^2)\frac{\partial^2 y}{\partial x'^2} - 2(x_{x'}x_{y'} + y_{x'}y_{y'})\frac{\partial^2 y}{\partial x'\partial y'} + (x_{x'}^2 + y_{x'}^2)\frac{\partial^2 y}{\partial y'^2} = 0 \quad (10)$$

Their solution gives the values of the physical co-ordinates (x,y) at all points of the transformed computational square domain. Following this procedure, the transformed momentum differential equation in the computational domain becomes:

$$(x_{y'}^2 + y_{y'}^2)\frac{\partial^2 v}{\partial x'^2} - 2(x_{x'}x_{y'} + y_{x'}y_{y'})\frac{\partial^2 v}{\partial x'\partial y'} + (x_{x'}^2 + y_{x'}^2)\frac{\partial^2 v}{\partial y'^2} + J^2 = 0 \quad (11)$$

The transformed partial differential equation (11) is discretized and solved using finite-difference techniques in the computational domain, for all grid points. Then the solution is simply transferred to the physical sinusoidal domain. Numerical computations were performed using a uniform 100×100 grid in x' and y'. The convergence criterion was set to 10^{-6} for the maximum relative error in values of the dependent variable between two successive iterations.

Numerical computations were carried out using double precision arithmetic in Fortran programming language.

4. Results

The results presented in this section, are obtained for incompressible fluid in developed slip flow. Though the Knudsen number should be classically limited in the range 10^{-3}–10^{-1}, also results with $Kn = 0.5$ are sketched. They can be seen as an extrapolation of slip flow in the early transition regime, or, if the hypothesis of Tison (1993), will be verified, as a solution in the extended region of slip flow. The numerical procedure reported in the preceding sections gives the 2D velocity distribution in the hydrodynamically developed region. The 2D distribution of the dimensionless shear stress $t = \tau a/\mu P$ is:

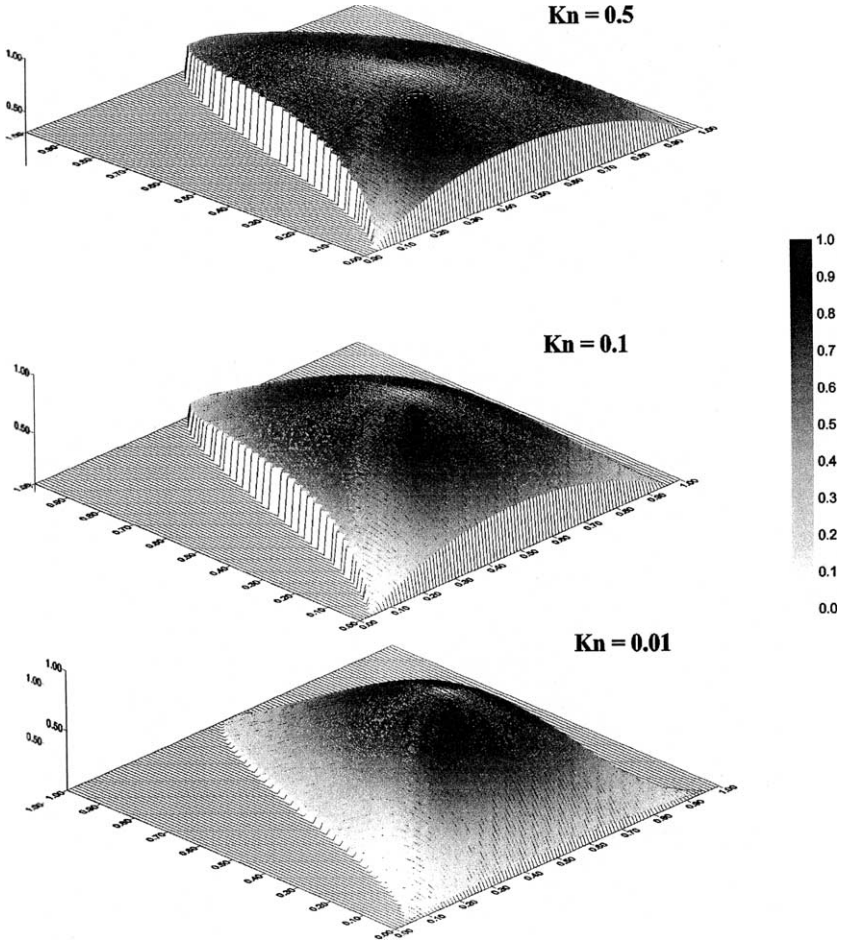

Fig. 2. Dimensionless velocity distribution, with $\beta = 1$.

$$t = \sqrt{v_x^2 + v_y^2} \tag{12}$$

where the partial derivatives of velocity with respect to the physical co-ordinates are:

$$v_x = \frac{v_{x'}x_{y'} - v_{y'}y_{x'}}{J}, \quad v_y = -\frac{v_{x'}x_{y'} - v_{y'}x_{x'}}{J} \tag{13}$$

In order to determine the frictional loss from the velocity distribution, the average velocity is calculated from its usual definition. As usual, it is presented as the friction factor–Reynolds number product:

$$f\,Re = -\frac{2D^2}{A}\int \frac{\partial(V/W)}{\partial n}\,\mathrm{d}P_w = \frac{2d^2}{U} \tag{14}$$

The explicit numerical solutions have been obtained using a PC class computer. As an example, the 2D computed velocity distributions V/V_{max}, given by the numerical procedure, is shown in Fig. 2 for different values of Kn, and $\beta = 1$. These profiles are well supported by the physical intuition. The fluid velocity experiences a slow and gradual increase from the walls to the centre; the jump at the walls is well evident, mainly for increasing Knudsen numbers, as well as the occurrence of a more flattened profile.

Table 1 shows the dimensionless co-ordinate $\eta_{max}/b = y_{max}/\beta$, where the local velocity presents its maximum value in the single sine-shaped duct; with increasing Knudsen number the peak point gets far from the straight line, mainly for high aspect ratios.

The dimensionless maximum velocity is reported in Fig. 3, as a function of the Knudsen number, for different geometrical configurations. Fig. 4 sketches the friction factor–Reynolds number product. The graphs confirm the physical deductions: when Re is settled, f decreases for increasing values of Kn and decreasing values of β.

These results can be compared with the available data quoted in literature (Pinazza and Spiga, 2000; Richardson et al., 2000; Shah and London, 1978) for $Kn = 0$, which constitute a benchmark to verify the reliability and accuracy of the numerical procedure; the agreement is perfect. As a further benchmark, the parameters

Table 1
Location η_{max}/b of the maximum velocity

β	Kn			
	0	0.01	0.1	0.5
0.125	0.494	0.494	0.494	0.494
0.250	0.480	0.480	0.480	0.480
0.500	0.430	0.430	0.430	0.441
0.750	0.375	0.375	0.375	0.397
1.000	0.337	0.337	0.348	0.370
1.500	0.272	0.272	0.282	0.315
2.000	0.232	0.232	0.251	0.285
4.000	0.155	0.155	0.163	0.195

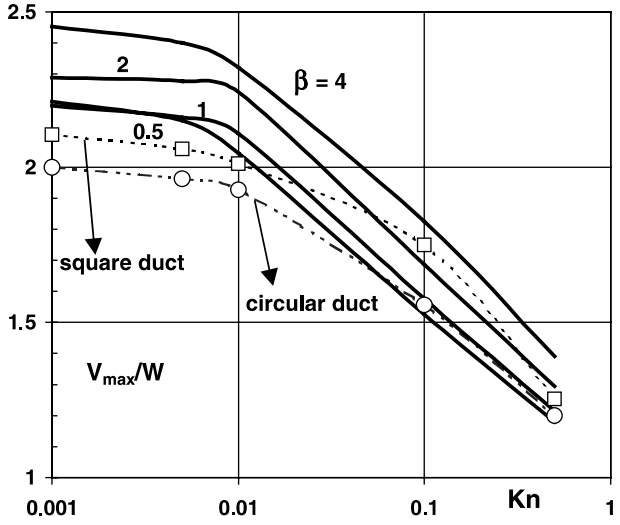

Fig. 3. Dimensionless maximum velocity.

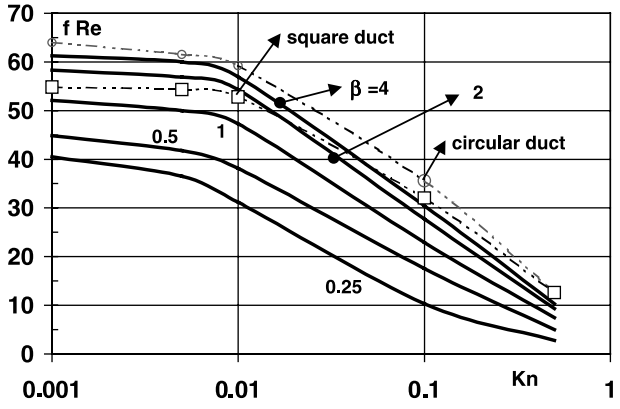

Fig. 4. Friction factor–Reynolds number product versus Kn.

V_{max}/W and $f\,Re$ can be deduced for slip flow in circular and square ducts (Morini and Spiga, 1998), they are sketched in Figs. 3 and 4 (dotted lines) and they show a trend very close to the behaviour of the analogous parameters for sine-shaped ducts.

Future works will be devoted to the solution of the Navier–Stokes equation with more general boundary conditions, considering a velocity-slip condition presented by Karniadakis and Beskok (2001), aimed at developing a unified flow model valid in the entire Knudsen regime. A semi-empirical model for rarefied flow in 3D ducts, proposed and validated by the same authors with a direct simulation Monte Carlo method, will be used for comparison with the numerical results.

Acknowledgements

Support from ASI, Italian Space Agency, is gratefully acknowledged (contract 003979 I/R/266/02).

References

Barron, R.F., Wang, X., Ameel, T.A., Warrington, R.O., 1997. The Graetz problem extended to slip flow. Int. J. Heat Mass Transfer 40, 1817–1823.

Beskok, A., Karniadakis, G.E., Trimmer, W., 1996. Rarefaction and compressibility effects in gas microflows. J. Fluid Eng. 118, 448–456.

Ding, J., Manglik, R.M., 1996. Analytical solutions for laminar fully developed flows in double-sine shaped ducts. Heat Mass Transfer 31, 269–277.

Haltiner, G.J., Williams, R.T., 1980. Numerical Prediction and Dynamic Meteorology. Wiley and Sons, New York.

Ho, C.M., Tai, Y.C., 1996. MEMS and its applications for flow control. J. Fluid Mech. 118, 437–447.

Hornbeck, R.W., 1975. Numerical Methods. Prentice-Hall, Englewood Cliffs, New Jersey.

Karniadakis, G.E., Beskok, A., 2001. Microflows: Fundamentals and Simulations. Springer, New York.

Kwang-Hua, W.C., 1999. Small-Knudsen-number flow in a corrugated tube. Meccanica 34, 133–136.

Larrodé, F.E., Housiadas, C., Drossinos, Y., 2000. Slip flow heat transfer in circular tubes. Int. J. Heat Mass Transfer 43, 2669–2680.

Manglik, R.M., Bergles, A.E., 1998. Numerical modeling and analysis of laminar flow heat transfer in non-circular compact channels. In: Sunden, B., Faghri, M. (Eds.), Computer Simulations in Compact Heat Exchangers. Computational Mechanics Publications, Southampton (UK).

Morini, G.L., Spiga, M., 1998. Slip-flow in rectangular microtubes. Microscale Therm. Eng. 2, 273–282.

Pinazza, O., Spiga, M., 2000. Laminar flow in corrugated single and double-sine shaped ducts. Trends Heat Mass Moment. Transfer 6, 71–79.

Richardson, D.H., Sekulic, D.P., Campo, A., 2000. Low Reynolds number flow inside straight micro channels with irregular cross sections. Heat Mass Transfer 36, 187–193.

Shah, R.K., London, A.L., 1978. Laminar Flow Forced Convection in Ducts. Academic Press, New York.

Thomson, J.F., Warsi, Z.U.A., Mastin, C.W., 1982. Boundary-fitted coordinate systems for numerical solution of partial differential equations—A review. J. Comput. Phys. 47, 1–108.

Tison, S.A., 1993. Experimental data and theoretical modeling of gas flows through metal capillary leaks. Vacuum 25, 151–156.

Uzun, I., Ünsal, M., 1997. A numerical study of laminar heat convection in ducts of irregular cross-sections. Int. Commun. Heat Mass Transfer 24, 835–848.